

1 **A study on the performance of low-cost sensors for source**
2 **apportionment at an urban background site**

3
4 **Dimitrios Bousiotis¹, David C.S. Beddows¹, Ajit Singh¹, Molly Haugen²,**
5 **Sebastián Diez³, Pete M. Edwards³, Adam Boies², Roy M. Harrison¹, and**
6 **Francis D. Pope^{1*}**
7

8 ¹Division of Environmental Health and Risk Management, School of Geography, Earth and
9 Environmental Sciences University of Birmingham, Edgbaston, Birmingham B15 2TT,
10 United Kingdom

11
12 ²Department of Engineering, University of Cambridge, Trumpington Street, Cambridge,
13 CB2 1PZ, United Kingdom

14
15 ³Wolfson Atmospheric Chemistry Laboratories, Department of Chemistry, University of
16 York, Heslington, York YO10 5DD, United Kingdom

17
18 *Corresponding Author, correspondence to Francis Pope f.pope@bham.ac.uk

19 **Abstract**

20 Knowledge of air pollution sources is important in policy making and air pollution mitigation,
21 Until recently, source apportion analyses were limited and only possible with the use of
22 expensive regulatory-grade instruments. In the present study we applied a two-step Positive
23 Matrix Factorisation (PMF) receptor analysis at a background site in Birmingham, UK using
24 data acquired by low-cost sensors (LCS). The application of PMF allowed for the
25 identification of the sources that affect the local air quality, clearly separating different
26 sources of particulate matter (PM) pollution. Furthermore, the method allowed for the
27 contribution of different air pollution sources to the overall air quality at the site to be
28 estimated, thereby providing pollution source apportionment. The use of data from
29 regulatory-grade (RG) instruments further confirmed the reliability of the results, as well as
30 further clarifying the particulate matter composition and origin. Comparing the results from
31 a previous analysis, in which a k-means clustering algorithm was used, a good consistency
32 between the k-means and PMF results was found in pinpointing and separating the sources
33 of pollution that affect the site. The potential and limitations of each method when used
34 with low-cost sensor data are highlighted. The analysis presented in this study paves the
35 way for more extensive use of LCS for atmospheric applications, receptor modelling and
36 source apportionment. Here, we present the infrastructure for understanding the factors
37 that affect air quality at a significantly lower cost that previously possible. This should
38 provide new opportunities for regulatory and indicative monitoring for both scientific and
39 industrial applications.

Deleted: While the measurements of atmospheric pollutants are useful in understanding the level of the air quality at a given area, receptor models are equally important in assessing the sources of these pollutants and the extent of their effect., ...

Deleted: This information is very

Deleted: helping

Deleted: in

Deleted: to

Deleted: dealing with

Deleted: problems

Deleted: Such analyses

Deleted: and were attempted until recently

Deleted: Using

Deleted: achieved,

Deleted: at the background site in Birmingham

Deleted: provided results that were consistent with a previous study at the site...

Deleted: the anticipated

Deleted: and p

Deleted: ,

Deleted: even though in different measuring periods, but also clearly separated the anticipated sources of particulate matter (PM) and pollution. Additionally

Deleted: Additionally

Deleted: supplied a metric

Deleted: us

Deleted: This was achieved even though the two studies occurred in different measuring periods., and Additionally, t

Deleted: and

Deleted: the

Deleted: ,

Deleted: can

Deleted: thus

Deleted: open

Deleted: ing

Deleted: up multiple

77 **1. Introduction**

78 Air pollution is a major problem not only affecting human health (Pascal et al., 2013; Rivas
79 et al., 2021; Shiraiwa et al., 2017; Wu et al., 2016; Zeger et al., 2008), but also causing
80 environmental deterioration and social disparity due to its effect on climate change
81 (Manisalidis et al., 2020; Mannucci and Franchini, 2017; Moore, 2009). Air pollution is
82 typically more problematic in urban environments which have multiple air pollution sources,
83 or locations near pollution hot spots (Valavanidis et al., 2008, Bousiotis et al., 2021). The
84 knowledge of air pollution sources is vital in understanding the air quality at a given site as
85 well as for policy making and action to improve air quality. Such knowledge was provided,
86 until recently, by the analysis of data from expensive regulatory grade (RG) instruments. The
87 use of RG instruments was not extensive due to their high cost and bulky size limiting their
88 use almost exclusively for scientific research. As a result, there is limited knowledge of the
89 sources that affect the air quality. This is in part due to the small number of deployments
90 and hence low spatial resolution of these expensive instruments (Kanaroglou et al., 2005),
91 especially in low- and middle-income countries. In these areas the problem of air quality and
92 its effect on human health is of great importance and expected to further increase in the
93 coming years as a result of their rapid industrial and population growth (Kan et al., 2009;
94 Petkova et al., 2013). To combat this, in the past decade, the development of low cost
95 sensors (LCS) measuring either PM or gas phase pollutant concentrations has intensified
96 (Lewis et al., 2018; Penza, 2019; Popoola et al., 2018). These LCS are still far from being an
97 equal alternatives to the more expensive RG instruments. Many limitations are associated
98 with their use, with the main shortcoming being the inconsistency of their measurements,
99 even for similar sensors deployed at the same site (Austin et al., 2015; Sousan et al., 2016),
100 either due to operational and detector sacrifices that allow them to be inexpensive or from
101 the effect of meteorological conditions that affect their measurements (Crilley et al., 2020;
102 Hagan and Kroll, 2020; Wang et al., 2021). Thus, consistent calibration (Kosmopoulos et al.,
103 2020; De Vito et al., 2020) and data corrections (Crilley et al., 2018; Liang et al., 2021; Vajs et
104 al., 2021) are required for these sensors to provide reliable measurements, although
105 sometimes even this is not enough (Giordano et al., 2021). Nevertheless, these sensors have
106 the potential to change the state of air pollution monitoring by allowing wider use and
107 better spatio-temporal coverage.

Deleted: This effect i

Deleted: more prominent especially within the

Deleted: , though areas even hundreds of kilometres away from the emission sources can also be affected

Deleted: As a result, t

Deleted: the sources of

Deleted: both

Deleted: now

Deleted: , t

Deleted: which

Deleted: almost

Deleted: exiguous

Deleted: , though

Deleted: being far from

Deleted: bias

Deleted: (

Deleted:) in addition to their continuous improvement and evolution...

126 Many applications of LCS have been found in recent years at sites that were previously
 127 inaccessible by regulatory instrumentation, either due to [them](#) being [cost prohibitive](#)
 128 (Miskell et al., 2018; Omokungbe et al., 2020; Pope et al., 2018), or due to their [physical size](#)
 129 limitations (Jovašević-Stojanović et al., 2015; Nagendra et al., 2019, Whitty et al., 2022).
 130 Additionally, the use of LCS made possible higher spatial resolution [measurements](#) than RG
 131 instruments (Feinberg et al., 2019; Krause et al., 2019; Prakash et al., 2021). [Thereby](#), greatly
 132 improving the ability to measure air quality at [multiple locations](#) of interest, even [down to](#)
 133 [the](#) neighbourhood scale (Schneider et al., 2017; Shafran-Nathan et al., 2019; Shindler,
 134 2021). [LCS have been shown to help supplement](#) existing regulatory networks (Weissert et
 135 al., 2020). While the applications of LCS provided the information of the level of air quality
 136 at more sites, [vital information on](#) air pollution sources and the environmental conditions
 137 that enable or [inhibit](#) air pollution, as well as their relative contributions is yet to be
 138 [exploited by LCS data](#), Pope et al., (2018) using PM ratios, managed to separate and identify
 139 the effect of major sources of pollution in several cities in East Africa [LCS data](#). Popoola et al,
 140 (2018) identified the sources of pollution near Heathrow Airport, London using a network of
 141 LCS. Bousiotis et al., (2021) using k-means clustering on PM data from both a LCS and an RG
 142 instrument, showed the strengths and limitations of the sensor, in measuring particle
 143 number concentrations and using them to identify the sources of pollution at a background
 144 site in Birmingham, UK. While these studies identified many sources and conditions that
 145 affect air quality, [they provided](#) no information on their temporal [variability](#) and [the](#) relative
 146 contributions [of different sources](#).
 147 In the present study, [a two-step PMF technique proposed by](#) Beddows and Harrison (2019),
 148 an advanced version of a statistical method for source apportionment successfully applied
 149 in many studies with RG instruments (Beddows et al., 2015; Harrison et al., 2011; Hopke,
 150 2016; Leoni et al., 2018; Pokorná et al., 2016), is applied on data collected from various LCS.
 151 This provides a quantitative separation of the different sources and their contributions to a
 152 background site located in Birmingham. Furthermore, data from RG instruments and an
 153 Aerosol Chemical Speciation Monitor (ACSM) were [used to provide further nuance to the](#)
 154 analysis. This was done not only to compare the results from the two sets, but to further
 155 characterise the sources of larger [sized](#) particles at the site as well. The results of the
 156 present analysis are also compared with those from a previous study at the same site made
 157 by Bousiotis et al., (2021) [using k-means clustering](#), displaying the additional information

Deleted: over the

Deleted: providing measurements

Deleted: economically difficult

Deleted: set by their size

Deleted: ,

Deleted: more points

Deleted: at

Deleted: , supplementing

Deleted: the

Deleted: the

Deleted: f

Deleted: disable

Deleted: uncovered by their use

Deleted: using data from

Deleted: ed the

Deleted: at the sites

Deleted: re was

Deleted: the

Deleted: (

Deleted: ,

Deleted: also

Deleted: in

180 provided by the PMF as well as to check the consistency of the results between the two
181 methods. To the authors' knowledge source apportionment with LCS data has only been
182 attempted previously by Hagan et al., (2019) using Non-negative Matrix Factorisation (NMF,
183 a version of PMF in which all components of the data matrix are weighted equally rather
184 than with individual errors) on a dataset from New Delhi, India. This study provided
185 information about combustion and non-combustion air pollution sources as well as their
186 partial contributions in a three-factor solution. The present work prepares the ground for
187 future use of source apportionment with LCS in a variety of scientific and industrial
188 scenarios. This will make more feasible their wider use, either as standalone air pollution
189 sources data sources, or in combination with RG instruments for increasing spatial coverage.

Deleted: NMF

Deleted: derivative

Deleted: ,

Deleted: ing

Deleted: of

Deleted: sets

Deleted: such

Deleted: sensors

Deleted: , which can m

Deleted: of the

Deleted: needed for such studies

Deleted: better

191 2. Methods

192 2.1 Location of the site and instruments

193 The measurement site is the Birmingham Air Quality Supersite (BAQS) located at the
194 grounds of the University of Birmingham (52.45°N; 1.93°W) (fig. 1). This is an urban
195 background site within a large residential area about 3 km southwest of the city centre of
196 Birmingham. For this site, PM concentration measurements in the range 0.35 to 40 µm were
197 collected using an Alphasense OPC-N3 in a 10 second resolution (averaged in 1-hour
198 resolution) for the period between 16/10/2020 to 30/10/2020. Additionally, data from
199 several LCS were also collected. NO, NO₂ and ozone measurements were collected using the
200 Box Of Clustered Sensors (BOCS, Smith et al., 2019) in the same time resolution, as well as
201 black carbon (BC) concentrations using the MA200 sensor by Magee Scientific. Finally, the
202 data for the lung deposited surface area (LDSA) of particles in the range of 10 nm to 10 µm,
203 which is found to strongly correlate with BC emissions (Lepistö et al., 2022), was collected
204 using a set of two Naneos Partectors by Naneos Particle Solutions GmbH. One sensor
205 measured the surface of all particles in this size range, while the second is placed after a
206 catalytic stripper (Catalytic Instruments CS015) which removes the semi-volatile particles
207 (Haugen et al. 2022).

Deleted: x

208 Apart from the data provided directly from the sensor before the catalytic stripper, the ratio
209 between the measurements of the two Naneos Partectors was also considered according to:

210

224
$$LDSA_{ratio} = \frac{LDSA \text{ after the catalytic stripper}}{LDSA \text{ before the catalytic stripper}}$$

225
226 This was done to resolve whether such a configuration can provide additional information
227 for the origin of pollution or the age of the pollutants in the incoming air masses, as
228 increased concentrations of semi-volatile compounds are usually associated with
229 anthropogenic sources, especially in the urban environment (Mahbub et al., 2011, Schnelle-
230 Kreis et al., 2007, Xu and Zhang, 2011). Thus, a high $LDSA_{ratio}$ is expected to be associated
231 with fresher pollution which usually has a higher content of volatile compounds (i.e.,
232 pollution sources at a close distance from the site), while lower ratios are probably
233 associated with either cleaner conditions or more regional and aged pollution with higher
234 concentrations of semi-volatile compounds, generally associated with sources at a greater
235 distance from the measuring site. This specific metric was also used in our previous study
236 (Bousiotis et al., 2021) and the consistency of the results between the two will be
237 compared.

238 For better characterisation of the larger particles, the Aerodyne ACSM was used, providing
239 information about its composition in the size range between 40 nm to 1 μm for NO_3^- , SO_4^{2-}
240 and organic content. For the comparison of the results, data from RG instruments were also
241 used, namely a Palas FIDAS (for PM), a Teledyne T500U (for NO_x), a Thermo 49i (for O_3) and
242 an AE33 aethalometer from Magee Scientific (for BC). Comparison of the regulatory
243 instruments and the LCS allows for consistency of the results between instrument types to
244 be checked. [A detailed description of the operation and more information about the sensors](#)
245 and instruments used in this study can be found in Bousiotis et al., (2021).

Deleted: M

Moved down [1]: Finally, for the present study the PMF analysis was performed using the second iteration of the PMF software developed by Paatero (2004a; 2004b). Data was analysed using the Openair package for R (Carlslaw and Ropkins, 2012), and back trajectory data were extracted by NOAA Air Resources Laboratory and calculated using the HYSPLIT model (Draxler and Hess, 1998).[¶]

246
247
248 **2.2 Positive Matrix Factorisation and data analysis**

249 The PMF is a multivariate data analysis, developed by Paatero (Paatero and Tapper, 1993;
250 1994), which is the most commonly used method for source apportionment and has been
251 applied numerous times in the field of aerosol science. The method is a weighted least-
252 squares technique that describes relationships among species measurements (Reff et al.,
253 2007). It assumes that X is a matrix of observed data, typically either particle number size

262 distributions (PNSDs) or chemical composition data, and u is the known matrix of the
263 experimental uncertainty of X . Both X and u are of dimensions $n \times m$ (where n is the number
264 of measurements and m is the number of species measured). The method solves the
265 bilinear matrix problem $X = GF + E$ where F is the unknown right hand factor matrix
266 (sources) of dimensions $p \times m$, G is the unknown left hand factor matrix (contributions) of
267 dimensions $n \times p$, and E is the matrix of residuals. The problem is solved in the weighted
268 least-squares sense: G and F are determined so that the Euclidean norm of E divided
269 (element-by-element) by u is minimized. Furthermore, the solution is constrained so that all
270 the elements of G and F are required to be non-negative (Paatero and Tapper, 1994). Higher
271 F values account for better association of the given variable with the factor it is assigned to,
272 while higher G values account for greater contribution of the factor at the given time period.

273 In the present analysis, a combination of both PNSD and particle composition data were
274 used. Such a combination may cause several shortcomings in the application of the PMF as
275 different types of data are used, due to the significant difference between the nature of
276 each variable. While this could be overcome by increasing the total weights of the primary
277 group of measurements (the one considered better in driving the model), this could be
278 problematic in the treatment and importance of the auxiliary dataset in the model
279 (Beddows and Harrison, 2019). To overcome these shortcomings the two-step PMF method,
280 proposed by Beddows and Harrison (2019), was used. In the first step of the method, a part
281 of the dataset is PMF-analysed (i.e. composition) and a solution is provided. The time series
282 G values (and errors) of the solution from the first step are then used as input variables to
283 the second step, where they are combined with the additional measurements (i.e. PNSD
284 data) dataset applying a second PMF analysis (a flow diagram of the method used as
285 presented by Beddows and Harrison, 2019 is found in figure S1). In the present study the
286 opposite path was considered, with the first step using the PNSD provided by the OPC
287 sensor and the inclusion of particle composition data in the second step. This was explicitly
288 done for two reasons: 1. to test the capabilities of the LCS in source apportionment, 2. to
289 connect specific PNSD profiles with specific pollution sources. Furthermore, on the second
290 step of the analysis detailed in Beddows and Harrison (2019) the explained variance of the
291 factors from the first step were maximised. This directly connects the additional variables in
292 the second step with the PNSD profiles found in the first step, excluding the possible factors

Moved (insertion) [2]

Deleted: PMF is a descriptive model having no objective criterion in the choice of the optimal number of factors (Paatero et al., 2002)....

Deleted:

297 formed with the data from the additional LCS data. In the present study, this step in this
298 method was omitted, as the aim is to present the results of the receptor model as they
299 occur in real life using a combination of LCSs measuring both particle number
300 concentrations and composition.

301 As PMF is a descriptive model there is no objective criterion in the choice of the optimal
302 number of factors (Paatero et al., 2002). In all cases several solutions were tested, and the
303 solution chosen was the one that provided factors with unique properties. Solutions with
304 additional factors provided no extra information on additional sources, rather the additional
305 factors separated factors that had already found into smaller groups with no significant
306 covariation.

Formatted: Normal, Space Before: Auto, After: Auto, Line spacing: single, Pattern: Clear (White)

307 For the study site, particle number concentration data were available from the OPC for
308 particles of diameter < 40 µm, but only data up to 10 µm were used. This was due to the
309 lack of sufficient non-zero counts in the larger size bins above that size threshold, which
310 disfavors PMF analysis to be completed. Additionally, separate LCS data for NO and NO₂
311 were available from the BOCS. The NO data showed sensible variation (which is the more
312 important factor in the PMF analysis), however, a great number of the NO data points had
313 low negative values due to their very low concentrations, which is impossible data for the
314 PMF algorithm. Rather than removing the negative numbers or artificially calibrating the
315 data upwards, we use NO_x (NO + NO₂) as the variable of interest.

316 Finally, to avoid the increased uncertainties from the use of unavailable data (as missing
317 data are treated with increased uncertainties), a time window for which all data were
318 available was chosen. Thus, data availability is 100% and no special treatment was
319 considered for missing data.

320 Finally, for the present study the PMF analysis was performed using the second iteration of
321 the PMF software developed by Paatero (2004a; 2004b). Data was analysed using the
322 Openair package for R (Carlslaw and Ropkins, 2012), and back trajectory data were
323 extracted by NOAA Air Resources Laboratory and calculated using the HYSPLIT model
324 (Draxler and Hess, 1998).

Moved (insertion) [1]

325

326

327 **3. Results**

328 **3.1 General conditions at the BAQS site and overall performance of the low-**
329 **cost sensors**

330 The measuring period (16th to 30th of October 2020) was chosen as it is a period which
331 presented rather typical meteorological conditions in the area, had no missing data from
332 any of the instruments used, and because they were the last days before the second
333 lockdown due to COVID-19 was applied (31st of October 2020). General meteorological
334 conditions were rather typical for the period in Birmingham, UK. As a result, the conditions
335 and activities in the surrounding area found in this period are considered almost consistent
336 with the normal conditions at the site in the autumn season. Mean temperature was $10.0 \pm$
337 2.5°C and mean relative humidity was $87.9 \pm 7.5 \%$ (standard deviations are calculated using
338 hourly data) during the measurement period. The average wind profile (Fig. S2) was also
339 typical for the UK with mainly southwestern winds of relatively low speed ($2.1 \pm 1.1 \text{ m s}^{-1}$).

340
341 Most of the LCS correlated well when compared to their more expensive RG counterparts,
342 using the Pearson correlation coefficient as the measure of correlation. The OPC-N3
343 presented a strong correlation for PM₁ ($r = 0.88$), though its performance weakened with
344 greater sized PM ($r = 0.49$ for PM_{2.5} and $r = 0.46$ for PM₁₀). The decreasing correlation from
345 PM₁ to PM_{2.5} to PM₁₀ is likely due to greater wall losses in the tubing for the bigger particles.
346 Strong correlations were also found from the BOCS sensors as well, with both O₃ and NO_x
347 concentrations presenting high r values when compared with their respective RG
348 instrument measurements (0.95 and 0.82 respectively). Finally, the BC measuring LCS
349 presented lower agreement with the measurements from the RG instrument, with a
350 Pearson correlation value of 0.40. It is noted, in the present study the absolute performance
351 of the LCS is not of great importance and thus it is not analysed in depth. For the PMF model
352 to present meaningful results the representation of the relative values and variability of the
353 variables is crucial instead, and this is thoroughly tested in the present study.”

354
355 **3.2 First step PMF analysis (PNSD analysis)**

356 Following the discussed methodology a 4-factor solution was chosen for this analysis. The
357 PNSD profiles of the factors found are presented in Figure S3. Due to the limited variation of

Deleted: .

Deleted: 1

Formatted: Font: Not Italic, Font colour: Text 1

Formatted: Font: Not Italic, Font colour: Text 1

Formatted: Font: Not Italic, Font colour: Text 1

Moved up [2]: PMF is a descriptive model having no objective criterion in the choice of the optimal number of factors (Paatero et al., 2002).

Deleted: A 4-factor solution was chosen for this analysis. This is due to the relatively limited period analysed as, as mentioned earlier, no significant variation was found in either the meteorological conditions or the sources that affected the air quality in the area. Solutions with additional factors were also attempted but these provided no extra information on additional sources, rather the additional factors separated factors that had already found into smaller groups with no significant covariation.

Deleted: mentioned

Deleted: 2

374 the PNSD profiles when presenting all the size bins available, making some of them appear
375 identical (i.e. Factor 2 and 3, due to the increasing particle number concentration as the size
376 decreases), the smallest particle diameter size bin at 400 nm (particle diameter range
377 between 350 to 460 nm) was removed to better present the variation on the larger sizes.
378 Thus, the particle profiles without the smallest available size are presented in Figure 2. The
379 profiles in the range between 500 nm to 10 µm for the four factors, associated with unique
380 formations extracted from the method are:

- 381 • Factor 1, that presents no significant peaks in the measured range of the OPC, but
382 does show a steady increasing trend with particle diameters below 1 µm
- 383 • Factor 2, with a distinct particle diameter peak at about 2 µm
- 384 • Factor 3, with a distinct particle diameter peak at about 2 µm and an increasing
385 trend below 750 nm
- 386 • Factor 4, accounting for particle diameter peaking at about 750 nm and 1.5 µm.

387

388 **3.3 Second step PMF with LCS data (LC analysis)**

389 The four-factor solution was also chosen in the second step analysis, for which the results of
390 the first step are combined with the additional particle and gas phase composition datasets
391 from LCS. The addition of more factors instead of adding information or providing clearer
392 associations with the factors from the first step, it separated the existing factors and their
393 association with the particle composition data into mixed factor groups with less significant
394 contributions of the variables. The association of the variables with each factor is presented
395 in figure 3, while the temporal variation of the contributions G of all the factors from this
396 analysis is presented in figure 4, along with the wind profile for some periods when each
397 factor was dominant.

398

399 The four new factors are:

400 **LC1 (Local and city centre pollution on calm conditions):** The LC1 is strongly associated with
401 the first factor from the initial PMF on the PNSD. For the period when the contribution of
402 this factor is higher (18th and 19th of October, see fig. 4) rather slow winds prevail from
403 many sectors (in this case mainly from the southwest). This factor has higher contributions
404 during calm conditions and during periods with north-eastern winds, though with lower

405 contribution (Fig. 5). It is highlighted that at the northeast of the specific site is the city
406 centre of Birmingham which is one of the main sources of pollution as found from a
407 previous study (Bousiotis et al., 2021). Looking at the diurnal variation (Fig. S4) of this factor
408 we see increased contributions during early morning and evening hours, likely associating it
409 with the morning and evening rush hours. The increased contributions during night-time
410 should not be overlooked and are probably the result of the lower boundary layer height
411 (BLH) during this time of the day. Additional data analysis shows an increased association of
412 this factor with PM₁ (Fig. 3), though this association is reduced for particles of larger sizes,
413 further confirming the lack of additional peaks on greater sizes. This along with the
414 increased association with the LDSA indicates the presence of large number of particles
415 below the detection limit of the instrument. This factor is also associated with almost all the
416 pollutants used, such as NO_x, CO and BC, though not as strongly as factor LC3 that is
417 discussed below, probably associated with pollution sources in a closer range to the
418 measuring station, as well as to a smaller extent with pollution from the city centre. Its
419 connection with air masses from the northeast is also confirmed from the back trajectory
420 analysis (Fig. 6), in which the highest contributions of this factor were found for air masses
421 from the northeast.

422 **LC2 (Marine):** This factor is strongly associated with the fourth PNSD factor from the initial
423 analysis (fig. 3). It presents relatively high association with PM which increases as the size
424 increases. No other significant association is found rather than relatively weak ones with
425 ozone, CO and the LDSA_{ratio}. It does not have a clear diurnal variation (fig. S4), though it has
426 slightly increased contributions during night-time. Higher contributions for this factor are
427 found with south and south-eastern winds of high speed (fig. 4 and 5). This can be seen in
428 Figure 4, where the highest contributions of this factor are associated with strong southern
429 winds. The marine nature of this factor is clearly highlighted through the back trajectory
430 analysis for this factor (Fig. 6) in which higher contributions are mostly found with air
431 masses originating from the north Atlantic Ocean, while some contributions from southern
432 Spain and Africa, which may be associated with Saharan dust and pollution from these
433 areas.

434 **LC3 (midday city centre and southwest pollution):** This factor does not have any significant
435 association with any of the factors from the PMF analysis of the PNSD (fig. 3). It presents
436 greater contributions during the midday (fig. S4), and it is associated with north-eastern and

Deleted: 3

Deleted: 3

Deleted: 3

440 southwestern winds (fig. 5). It has high contributions with all the pollutants included in the
441 analysis and the $LDSA_{ratio}$, which points to fresher pollution (pollution sources closer to the
442 measuring station). Such sources of pollution in most cases are associated with particles of
443 sizes smaller than that measured by the OPC, hence the lack of association with any of the
444 factors found from the PNSD analysis. The back trajectory analysis provides no clear origin
445 for the air masses of this factor (fig. 6), which may indicate a relatively smaller pollution
446 lifetime, which is associated with incoming air masses from all directions.

447 **LC4 (Urban background):** This factor has a rather strong association with the second factor
448 from the PNSD analysis and a weaker one with the third one (Fig. 3). It does not have a clear
449 diurnal variation (fig. S4) and it is mainly associated with north-eastern winds (Fig. 5). It
450 presents weak associations with all the variables inputted in the PMF analysis making it hard
451 to distinguish either a source or conditions for which this factor is enhanced. The back
452 trajectory analysis though shows that this factor is associated with air masses from
453 continental Europe as well as Scandinavia (Fig. 6), which for the UK, usually contain aged
454 and hence typically larger secondary PM pollutants.

455

456 **3.4 Second step PMF with RG data (RG analysis)**

457 While the primary aim of the present study is to highlight the capabilities of LCS in source
458 apportionment, the measurements provided by these devices are mainly focused on gas
459 phase pollutants which are in most cases associated solely with ultrafine particles. The OPC
460 measurements used for this site have a particle diameter range between 400 nm to 10 μm .
461 Thus, apart from using data from RG instruments measuring gas phase pollutants, it was
462 considered sensible to add data from an ACSM, which measures compounds associated with
463 larger particles, such as nitrate, sulphate, and organic compounds (used in this analysis).
464 Some of the factors in this analysis are rather similar with those formed from the analysis
465 using LCS dataset. Thus, the **RG1** factor in this analysis is mainly associated with the first
466 factor from the PNSD analysis in the first step (Fig. 7), similar to that found also in LC1 (Fig.
467 3). The wind conditions are also similar for which these factors from the two analyses
468 present their highest contribution (Fig. 8), as well as their temporal variation (Fig. S5) and
469 diurnal variation (Fig. S6). The additional information granted using the ACSM data is the
470 strong association of this factor with nitrate, and a stronger association with NO_x and BC are

Deleted: 3

Deleted: 4

Deleted: 5

474 also found, compared to the LC analysis. This further associates this factor with nearby
475 sources of pollution which prevail with low wind speeds and may associate the conditions of
476 this factor with the low BLH height found during that time, though high contributions were
477 also found for early morning and evening hours, as in the LC analysis for the similar factor.
478 Finally, the back trajectory analysis (fig. 9) shows higher contributions associated with air
479 masses from the northeast, further confirming its similarity with the first factor from the LC
480 analysis and its urban origins.

481 The **RG2** is unique and has no association with the factors from the PMF on PNSD data and
482 is strongly associated only with sulphate (Fig. 7). It does not have a clear diurnal variation
483 (fig. S6) and seems to have higher contributions with southwestern winds of rather high
484 speed and to a lesser extent with north-easterly winds (Fig. 8). The back trajectory analysis
485 (Fig. 9), while presenting few relatively high contributions from continental Europe, mainly
486 associates this factor with incoming air masses from all sea origins surrounding the UK. This
487 is expected as the ocean is a source of sulphate containing compounds (for the particles at
488 the size range measured by the OPC), either sea-salt sulphate or marine biogenic sulphate
489 (Lin et al., 2012; Raes et al., 2000).

490 The **RG3** is similar to the LC2 and is mainly associated with the fourth factor from the PNSD
491 analysis and to a lesser extent with the third (Fig. 7). This factor has slightly increased
492 contributions during night-time (Fig. S6) and south and southwestern winds (Fig. 8). It
493 presents increased associations with increasing PM size, though in this case it is also
494 strongly associated with O₃. Unfortunately, no Cl or Na data were available to further
495 determine the marine nature of this factor. The back trajectory analysis though once again
496 presents higher contributions with marine air masses (Fig. 9), though some hot spots are
497 also found from continental Europe, which probably explain to an extent the small
498 associations found with NO_x and organic compounds from the ACSM.

499 Finally, the **RG4** is mainly associated with the second factor and to a lesser extent with the
500 third from the PNSD analysis (Fig. 7). It presents higher contributions with north-eastern
501 winds (Fig. 8), has an unclear diurnal variation (Fig. S6), and presents higher contributions
502 with air masses from continental Europe (Fig. 9), like the LC4 from the second-step analysis.
503 While in that analysis it was difficult to characterise the sources for that factor, the strong
504 association with organic compounds found here with the addition of the ACSM data helps in
505 its clearer characterisation.

Deleted: 5

Deleted: 5

Deleted: 5

509

510 **4. Discussion**

511 **4.1 Comparison of the results from the second-step analysis**

512 It should be noted that regardless of any possible similarities between the two (second-
513 step) analyses, a direct comparison of the results should be conducted with great care. As
514 different variables are considered, even minor differences may result in different trends,
515 contribution of variables and the sources described. Regardless, the results of the two
516 analyses have great similarities especially on specific factors that are associated with the
517 same particle size distribution profiles (from the PNSD analysis), contribution of chemical
518 compounds and diurnal variation. Three factors were found to have great similarities and
519 were associated with similar particle profiles. Specifically, these are the factors describing
520 the sources of particles which are either in close proximity to the measuring station or occur
521 with almost calm conditions (Factor 1 on both analyses), the marine factor (Factor 2 on LC
522 analysis and 3 on RG analysis) and the continental factor (Factor 4 on both analyses).

523 Looking at their temporal contributions (Fig. 4 and S5), the first factors on both analyses
524 appear to consistently peak on periods when the second set of factors (LC2 and RG3)
525 presents lower G contributions (and vice versa), which is expected due to the nature of their
526 sources. The factors on both sets though have almost identical temporal variation of their G
527 contributions regardless of the dataset. For the fourth factors on both analyses, though
528 presenting similar associations with their variables, differences are found in their temporal
529 variations with the addition of the ACSM data. This shows that while these factors appear to
530 be almost identical, small differences can still be found in their temporal variation and
531 variable associations, when different datasets are considered. Nevertheless, the addition of
532 the ACSM data shows a very high contribution of NO_3^- on the first RG factor, SO_4^{2-} for the
533 second factor and the organic component on the fourth factor.

534 The remaining factor from both analyses though is completely different between the two
535 analyses and point towards the differences on the variables used for each. In the LC analysis
536 the factor formed consists of sources that are associated with fresher pollution sources.
537 Thus, a factor with strong associations with all the pollutants available was formed, it was
538 not associated with any of the PNSD formations from the first-step analysis and presented a
539 unique diurnal variation peaking midday. This should be expected as the particle size

Deleted: 4

541 measured by the OPC is much larger compared to the size of the particles these chemical
542 compounds are usually associated with. The occurrence of this factor was probably included
543 partially to the first and fourth factor of the RG analysis, as these present relatively higher
544 associations with NO_x and BC and more enhanced contributions during midday hours
545 compared to their LC analysis counterparts.
546 Finally, using the RG instrument data, the additional factor is associated with sulphate
547 alone. This is a result that was consistent regardless of the number of factors used, either
548 greater or smaller. Sulphate containing compounds have a lower volatility compared to the
549 other chemical compounds used in the analysis and is relatively more stable with a rather
550 small seasonal variation (Utsunomiya and Wakamatsu, 1996), thus having a longer lifespan
551 and distance of travel. As a result, sulphate was found not to be associated with any other
552 chemical compound and always formed a factor of its own (regardless of the number of
553 factors chosen).

554

555 **4.2 Comparison with the results from a previous study.**

556 Although different methodologies were used with the previous analysis for the BAQS site
557 (Bousiotis et al., 2021), as well as for different time periods, many similarities were found
558 for the sources of particles at the site. The main source of smaller particles at the site in the
559 previous analysis is found to be the city centre in the northeast, for which relatively high
560 concentrations of NO_x were found. Similar is the case in the present analysis, as for the
561 sources found to be associated with north-easterly winds an association was also found with
562 NO_x and the LDSA_{ratio}. Additionally, a source of sulphate found with southerly winds was also
563 confirmed in the present study, with the association of high sulphate concentrations with a
564 factor, which presents higher contributions with winds from the southern sector. While in
565 the previous analysis the sources responsible for this source could not be pinpointed, in the
566 present analysis, using a back trajectory analysis, the sulphate factor was associated with
567 marine particle sources from all directions. Furthermore, a factor in the present analysis,
568 which identifies hot spots south of the measuring station with strong presence of PM of all
569 sizes, was also found with the k-means analysis in the previous study, though in that case it
570 was more associated with the pollution sources from that side rather than the long-range
571 transport found here.

572 These similarities are very encouraging, as even though the analyses were made for
573 different periods and using different methods, there is consistency between the results. This
574 means that regardless of the different seasons studied (previous analysis was performed
575 during winter to early spring), the sources of particles (and pollution) are relatively uniform,
576 without significant changes.

577 Additionally, the k-means method identified sets of conditions that either promote or
578 suppress the pollution at the sites (as this can be illustrated with the variable particle
579 concentrations between the clusters found from the analysis), rather than separate sources
580 of pollution that affect the site. While this provides a more realistic picture of the conditions
581 it makes it harder to distinguish the specific sources and their effect in its air quality. On the
582 other hand, the PMF not only provides clearer separation of the sources, but the temporal
583 contribution of each source as well, which shows the real extent of the effect of each source
584 of particles or pollutants, thus achieving source apportionment rather than just the
585 identification of pollution sources that the k-means offers. The k-means approach identifies
586 the effect of the sources of particles, but it also separates cleaner periods as separate
587 clusters. These two effects gives a more complete overall picture of the air quality at a site.
588 PMF could also provide this information, but it would be more difficult to obtain looking at
589 the different sources and the conditions that keep them to low contributions (this would
590 also require a much greater number of factors).

591 Furthermore, due to the complexity of the clusters from the k-means, pinpointing the
592 sources that the particles are associated with is difficult. This is due to the clusters, being a
593 set of different sources and conditions rather than clearly separated sources, were not
594 clearly associated with distinct wind directions, speeds or hot-spots. Contrary to that, the
595 factors formed by the PMF present clearer association with specific sectors, thus making it
596 easier to define the sources associated with them, as in the results they are presented as
597 hot spots within the polar plots.

598 The analysis of atmospheric data using either k-means or PMF are proven to provide
599 adequate and trustworthy information for the sources of particles and by extension of
600 pollution at a site, even with the sole use of LCS as shown in this paper and the preceding
601 Bousiotis et al. 2021 paper. The combined use of both approaches provides a clearer picture
602 of the different sources and their effect, as the PMF is able to better separate and provide
603 the effect of the sources of pollution that affect the air quality at a site and the k-means

604 provides a more realistic representation of the conditions at a site, by showing the
605 combined effect of these sources. The relative consistency of the results found between the
606 two analyses, even being in different time periods, is very encouraging and shows that the
607 very important information of pollution receptor modelling is viable with LCS, providing a
608 much-needed alternative for countries or scenarios where the use of regulatory-grade
609 instruments is not feasible. The significantly lower price point of LCSs means that in addition
610 to hyperlocal measurement of air pollution, it should now be possible to deliver hyperlocal
611 source apportionment of air pollution though as highlighted within this study, there are
612 some limitations for specific sources associated with pollutants with certain properties.
613 Further exploration of these limitations and design of methodologies to overcome them,
614 can enhance their capability and open new research and industrial abilities to pinpoint air
615 pollution sources and subsequently manage them.

616 Finally, the $LDSA_{ratio}$, a variable that was introduced in the previous analysis, was included in
617 the present one as well. As in the previous analysis, this ratio was found to be more
618 associated with fresher pollution from combustion sources near to the measuring station,
619 for which it has reliably performed in both analyses.

620

621 5. Conclusions

622 To solve air quality problems and to deliver the associated policy making effectively, it is
623 vital to have a methodology to measure the sources of air pollution, and their relative
624 importance. Historically, this has been achieved using expensive RG instruments. The cost
625 implications of these studies make assessment at dense spatial resolutions limited. In this
626 study, data from a low-cost OPC and other LCS, measuring gas phase pollutants, black
627 carbon and the lung deposited surface area of particles in BAQS were analysed using the
628 two-step PMF analysis. Four factors were formed from this analysis and were associated
629 with their respective sources and to a great extent with unique PNSD profiles. The following
630 factors were found: a factor associated with either combustion sources in close proximity of
631 the measurement site or associated with calm conditions, a marine factor, a factor
632 associated with midday activities from the city centre and a more constant factor from the
633 northeast. The same analysis was also performed using data from RG instruments and the
634 same PNSD factors. This was done to evaluate the results from the low-cost sensor analysis,

Formatted: Font colour: Text 1

Formatted: Font: Not Italic, Font colour: Text 1

Formatted: Font: Not Italic, Font colour: Text 1

Deleted: , though as pointed by the present study with some limitations for specific sources associated with pollutants with certain properties. Further exploring these limitations and ways to overcome them, can enhance their This capability and will open new research and industrial abilities to pinpoint air pollution sources and subsequently manage them....

642 as well as to further characterise and clarify the sources associated with the factors formed.
643 Significant agreement was found between the results of the two analyses, highlighting that
644 the LCS are capable for carrying out such analyses. The additional ACSM data from the
645 second analysis further helped in the characterisation of the composition of the particles of
646 each factor, clarifying the sources associated with nitrate, sulphate and organic compounds
647 at the site, as well as strongly associating some with unique PNSD profiles. While in their
648 present state, the LCSs do not possess the full capability of the RG instruments for providing
649 high accuracy measurements, considering the limitations they were found to be adequate in
650 providing with the trends of the particles and pollutants measured which are important for
651 source apportionment studies. This is done at a fraction of the equipment cost; see
652 Bousiotis et al. 2021 for cost estimates.

653 Furthermore, comparing the results from the PMF to those from the k-means analysis
654 showed the different strengths and weaknesses of each approach. The PMF is better in
655 pinpointing the effect of separate sources of pollution, but it is difficult to give a clear
656 representation of the actual conditions when each factor affects the site. The k-means is not
657 as efficient in clearly separating the different sources, but it does provide a more realistic
658 picture of the air quality at a site in relation to the ambient conditions. The combined use of
659 both methods though provided a clearer picture for the conditions at the site.

660 The methodologies developed and used in this study will help to reliably facilitate source
661 apportionment studies in the future, with either the sole use of LCS or their combination
662 with RG instruments. As for a given site, specific PNSD formations are associated with
663 specific conditions and sources (Harrison et al., 2011), by creating a repository of unique
664 PNSDs at a site and associating them with their respective sources, in the future the source
665 apportionment may be done to an extent using only PNSD profiles and meteorological data
666 alone. This will do much in simplifying the source apportionment process allowing its wider
667 application and help in dealing with environmental challenges, though it can be challenging
668 in sites with particle emissions smaller than what the OPC can measure (ex. vehicle exhaust
669 emissions). For this though, further testing in more diverse environments and scenarios is
670 needed which, along with the anticipated development of the LCS, will provide a denser and
671 reliable measuring network even for countries with lower incomes and help for cleaner and
672 healthier environmental conditions.

673

674

675 **Author Contributions**

676 The study was conceived and planned by FDP who also contributed to the final manuscript,
677 and DB who carried out the analysis and prepared the first draft. AS, MH, DCSB and SD
678 provided data for the analysis. DCSB provided help with the analysis of the data. RMH, PME
679 and AB contributed to the final manuscript.

680

681 **Competing Interests**

682 The authors have no conflict of interests.

683

684 **Acknowledgements**

685 We thank the OSCA team (Integrated Research Observation System for Clean Air) at the
686 Birmingham Air Quality Supersite (BAQS), funded by NERC (NE/T001909/1), for help in data
687 collection for the regulatory-grade instruments. We thank Lee Chapman for access to his
688 meteorological dataset used in the analysis.

689 **Financial support.**

690 This research has been supported by the Natural Environment Research Council (NERC grant
691 no. NE/T001879/1), the Engineering and Physical Sciences Research Council (EPSRC grant
692 no. EP/T030100/1) and internal EPSRC funding provided to the University of Birmingham for
693 Impact Acceleration.

694

695

696 **References**

697

698 Austin, E., Novosselov, I., Seto, E. and Yost, M. G.: Laboratory evaluation of the Shinyei

699 PPD42NS low-cost particulate matter sensor, *PLoS One*, 10(9), 1–17,

700 doi:10.1371/journal.pone.0137789, 2015.

701

702 Beddows, D. C. S., Harrison, R. M., Green, D. C. and Fuller, G. W.: Receptor modelling of both

703 particle composition and size distribution from a background site in London, UK, *Atmos.*

704 *Chem. Phys.*, 15(17), 10107–10125, doi:10.5194/acp-15-10107-2015, 2015.

705

706 Beddows, D.C.S., and Harrison, R.M.: Receptor modelling of both particle composition and

707 size distribution from a background site in London, UK – a two-step approach, *Atmos. Chem.*

708 *Phys.*, 19, 39 – 55, <https://doi.org/10.5194/acp-19-39-2019>, 2019.

709

710 Bousiotis, D., Pope, F.D., Beddows, D.C.S., Dall'Osto, M., Massling, A., Nøjgaard, J.K.,

711 Nordstrøm, C., Niemi, J.V., Portin, H., Petäjä, T., Perez, N., Alastuey, A., Querol, X.,

712 Kouvarakis, G., Mihalopoulos, N., Vratolis, S., Eleftheriadis, K., Wiedensohler A., Weinhold,

713 A., Merkel, M., Tuch, T. and Harrison R.M.: A phenomenology of new particle formation

714 (NPF) at 13 European sites, *Atmos. Chem. Phys.*, 21, 11905 - 11925,

715 <https://doi.org/10.5194/acp-21-11905-2021> 2021.

716 Bousiotis, D., Singh, A., Haugen, M., Beddows, D.C.S., Diez, S., Edwards, P.M., Boies, A.,

717 Harrison, R.M. and Pope, F.D.: Assessing the sources of particles at an urban background site

718 using both regulatory grade instruments and low-cost sensors – A comparative study,

719 *Atmos. Meas. Tech.*, 14, 4139 – 4155, <https://doi.org/10.5194/amt-14-4139-2021>, 2021.

720

721 Carslaw, D. C. and Ropkins, K.: openair — An R package for air quality data analysis, *Environ.*

722 *Model. Softw.*, 27–28, 52–61, doi:10.1016/j.envsoft.2011.09.008, 2012.

723

724 Crilley, L. R., Shaw, M., Pound, R., Kramer, L. J., Price, R., Young, S., Lewis, A. C., and Pope, F.

725 D.: Evaluation of a low-cost optical particle counter (Alphasense OPC-N2) for ambient air

726 monitoring, *Atmos. Meas. Tech.*, 11, 709–720, <https://doi.org/10.5194/amt-11-709-2018>,
727 2018.
728

729 Crilley, L. R., Singh, A., Kramer, L. J., Shaw, M. D., Alam, M. S., Apte, J. S., Bloss, W. J.,
730 Hildebrandt Ruiz, L., Fu, P., Fu, W., Gani, S., Gatari, M., Ilyinskaya, E., Lewis, A. C., Ng'ang'a,
731 D., Sun, Y., Whitty, R. C. W., Yue, S., Young, S. and Pope, F. D.: Effect of aerosol composition
732 on the performance of low-cost optical particle counter correction factors, *Atmos. Meas.*
733 *Tech.*, 13(3), 1181–1193, doi:10.5194/amt-13-1181-2020, 2020.
734

735 Draxler, R. R. and Hess, G. D.: An Overview of the HYSPLIT_4 Modelling System for
736 Trajectories, Dispersion, and Deposition, *Aust. Meteorol. Mag.*, 47(January), 295–308, 1998.
737

738 De Vito, S., Esposito, E., Castell, N., Schneider, P. and Bartonova, A.: On the robustness of
739 field calibration for smart air quality monitors, *Sensors Actuators, B Chem.*, 310(July 2019),
740 127869, doi:10.1016/j.snb.2020.127869, 2020.
741

742 Feinberg, S. N., Williams, R., Hagler, G., Low, J., Smith, L., Brown, R., Garver, D., Davis, M.,
743 Morton, M., Schaefer, J. and Campbell, J.: Examining spatiotemporal variability of urban
744 particulate matter and application of high-time resolution data from a network of low-cost
745 air pollution sensors, *Atmos. Environ.*, 213(May), 579–584,
746 doi:10.1016/j.atmosenv.2019.06.026, 2019.

747 Giordano, M.R., Malings, C., Pandis, S.N., Presto, A.A., McNeill, V.F., Westervelt, D.M.,
748 Beekmann, M., and Subramanian, R.: From low-cost sensors to high-quality data: A
749 summary of challenges and best practices for effectively calibrating low-cost particulate
750 matter mass sensors, *Journal of Aerosol Science*,
751 <https://doi.org/10.1016/j.jaerosci.2021.105833>, 2021.

752 Hagan, D. H., Gani, S., Bhandari, S., Patel, K., Habib, G., Apte, J. S., Hildebrandt Ruiz, L. and
753 Kroll, J. H.: Inferring Aerosol Sources from Low-Cost Air Quality Sensor Measurements: A
754 Case Study in Delhi, India, *Environ. Sci. Technol. Lett.*, 6(8), 467–472,
755 doi:10.1021/acs.estlett.9b00393, 2019.

756

757 Hagan, D. and Kroll, J.: Assessing the accuracy of low-cost optical particle sensors using a
758 physics-based approach, *Atmos. Meas. Tech. Discuss.*, 1–36, doi:10.5194/amt-2020-188,
759 2020.

760

761 Harrison, R. M., Beddows, D. C. S. and Dall'Osto, M.: PMF analysis of wide-range particle size
762 spectra collected on a major highway, *Environ. Sci. Technol.*, 45(13), 5522–5528,
763 doi:10.1021/es2006622, 2011.

764

765 Haugen, M.J., Singh, A., Bousiotis, D., Pope, F.D., Boies, A.M.: Demonstrating the ability to
766 differentiate between semi-volatile and solid particle events with low-cost lung-deposited
767 surface area and black carbon particle sensors, *Atmosphere*, [13](https://doi.org/10.3390/atmos13050747), 747,
768 doi:10.3390/atmos13050747, 2022.

769

770 Hopke, P. K.: Review of receptor modeling methods for source apportionment, *J. Air Waste*
771 *Manag. Assoc.*, 66(3), 237–259, doi:10.1080/10962247.2016.1140693, 2016.

772

773 Jovašević-Stojanović, M., Bartonova, A., Topalović, D., Lazović, I., Pokrić, B. and Ristovski, Z.:
774 On the use of small and cheaper sensors and devices for indicative citizen-based monitoring
775 of respirable particulate matter, *Environ. Pollut.*, 206, 696–704,
776 doi:10.1016/j.envpol.2015.08.035, 2015.

777

778 Kan, H., Chen, B. and Hong, C.: Health impact of outdoor air pollution in China: Current
779 knowledge and future research needs, *Environ. Health Perspect.*, 117(5), 12737,
780 doi:10.1289/ehp.12737, 2009.

781

782 Kanaroglou, P. S., Jerrett, M., Morrison, J., Beckerman, B., Arain, M. A., Gilbert, N. L. and
783 Brook, J. R.: Establishing an air pollution monitoring network for intra-urban population
784 exposure assessment: A location-allocation approach, *Atmos. Environ.*, 39(13), 2399–2409,
785 doi:10.1016/j.atmosenv.2004.06.049, 2005.

786

787 Kosmopoulos, G., Salamalikis, V., Pandis, S. N., Yannopoulos, P., Bloutsos, A. A. and

Formatted: Normal (Web), Widow/Orphan control, Adjust space between Latin and Asian text, Adjust space between Asian text and numbers

Deleted: in submission

Formatted: Font: (Default) Calibri, 12 pt, Do not check spelling or grammar

789 Kazantzidis, A.: Low-cost sensors for measuring airborne particulate matter: Field evaluation
790 and calibration at a South-Eastern European site, *Sci. Total Environ.*, 748(October), 141396,
791 doi:10.1016/j.scitotenv.2020.141396, 2020.

792

793 Krause, A., Zhao, J. and Birmili, W.: Low-cost sensors and indoor air quality: A test study in
794 three residential homes in Berlin, Germany, *Gefahrstoffe Reinhaltung der Luft*, 79(3), 87–94,
795 doi:10.37544/0949-8036-2019-03-49, 2019.

796

797 Leoni, C., Pokorná, P., Hovorka, J., Masiol, M., Topinka, J., Zhao, Y., Křůmal, K., Cliff, S.,
798 Mikuška, P. and Hopke, P. K.: Source apportionment of aerosol particles at a European air
799 pollution hot spot using particle number size distributions and chemical composition,
800 *Environ. Pollut.*, 234, 145–154, doi:10.1016/j.envpol.2017.10.097, 2018.

801

802 Lepistö, T., Kuuluvainen, H., Lintusaari, H., Kuitinen, N., Salo, L., Helin, A., Niemi, J.V.,
803 Manninen, H.E., Timonen, H., Jalava, P., Saarikoski, S. and Rönkkö, T.: Connection between
804 lung deposited surface area (LDSA) and black carbon (BC) concentrations in road traffic and
805 harbour environments, *Atmospheric Environment*, 272, 118931,
806 <https://doi.org/10.1016/j.atmosenv.2021.118931>, 2022.

807

808 Lewis, A. C., von Schneidmesser, E., Peltier, R. E., Lung, C., Jones, R., Zellweger, C.,
809 Karppinen, A., Penza, M., Dye, T., Hüglin, C., Ning, Z., Leigh, R., Hagan, D. H., Laurent, O. and
810 Carmichael, G.: Low-cost sensors for the measurement of atmospheric composition:
811 overview of topic and future applications. [online] Available from:
812 http://www.wmo.int/pages/prog/arep/gaw/documents/Draft_low_cost_sensors.pdf, 2018.

813

814 Liang, Y., Wu, C., Jiang, S., Li, Y. J., Wu, D., Li, M., Cheng, P., Yang, W., Cheng, C., Li, L., Deng,
815 T., Sun, J. Y., He, G., Liu, B., Yao, T., Wu, M. and Zhou, Z.: Field comparison of
816 electrochemical gas sensor data correction algorithms for ambient air measurements,
817 *Sensors Actuators, B Chem.*, 327(November 2020), doi:10.1016/j.snb.2020.128897, 2021.

818

819 Lin, C. T., Baker, A. R., Jickells, T. D., Kelly, S. and Lesworth, T.: An assessment of the
820 significance of sulphate sources over the Atlantic Ocean based on sulphur isotope data,

821 Atmos. Environ., 62, 615–621, doi:10.1016/j.atmosenv.2012.08.052, 2012.
822

823 Mahbub, P., Ayoko, G.A., Goonetilleke, A., Egodawatta, P.: Analysis of the build-up of semi
824 and non volatile organic compounds on urban roads, Water Res. 45(9), 2835 - 2844, doi:
825 10.1016/j.watres.2011.02.033, 2011.
826

827 Manisalidis, I., Stavropoulou, E., Stavropoulos, A. and Bezirtzoglou, E.: Environmental and
828 Health Impacts of Air Pollution: A Review, Front. Public Heal., 8(February), 1–13,
829 doi:10.3389/fpubh.2020.00014, 2020.
830

831 Mannucci, P. M. and Franchini, M.: Health effects of ambient air pollution in developing
832 countries, Int. J. Environ. Res. Public Health, 14(9), 1–8, doi:10.3390/ijerph14091048, 2017.
833

834 Miskell, G., Salmond, J. A. and Williams, D. E.: Use of a handheld low-cost sensor to explore
835 the effect of urban design features on local-scale spatial and temporal air quality variability,
836 Sci. Total Environ., 619–620, 480–490, doi:10.1016/j.scitotenv.2017.11.024, 2018.
837

838 Moore, F. C.: Climate change and air pollution: Exploring the synergies and potential for
839 mitigation in industrializing countries, Sustainability, 1(1), 43–54, doi:10.3390/su1010043,
840 2009.
841

842 Nagendra, S., Reddy Yasa, P., Narayana, M., Khadirnaikar, S. and Pooja Rani: Mobile
843 monitoring of air pollution using low cost sensors to visualize spatio-temporal variation of
844 pollutants at urban hotspots, Sustain. Cities Soc., 44(September 2018), 520–535,
845 doi:10.1016/j.scs.2018.10.006, 2019.
846

847 Omokungbe, O. R., Fawole, O. G., Owoade, O. K., Popoola, O. A. M., Jones, R. L., Olise, F. S.,
848 Ayoola, M. A., Abiodun, P. O., Toyeye, A. B., Olufemi, A. P., Sunmonu, L. A. and Abiye, O. E.:
849 Analysis of the variability of airborne particulate matter with prevailing meteorological
850 conditions across a semi-urban environment using a network of low-cost air quality sensors,
851 Heliyon, 6(6), e04207, doi:10.1016/j.heliyon.2020.e04207, 2020.
852

853 Paatero, P. and Tapper, U.: Analysis of different modes of factor analysis as least squares fit
854 problems, *Chemom. Intell. Lab. Syst.*, 18(2), 183–194, doi:10.1016/0169-7439(93)80055-M,
855 1993.

856

857 Paatero, P. and Tapper, U.: Positive Matrix Factorization : A Non-negative factor model with
858 optimal utilization of error estimates of data values, *Environmetrics*, 5(April 1993), 111–126,
859 1994.

860

861 Paatero, P., Hopke, P. K., Song, X.-H., and Ramadan, Z.: Understanding and controlling
862 rotations in factor analytic models, *Chemometr. Intell. Lab.*, 60, 253–264, 2002.

863

864 Paatero P.: User's guide for positive matrix factorization programs PMF2 and PMF3, Part1:
865 tutorial. University of Helsinki, Helsinki, Finland, 2004a.

866

867 Paatero P.: User's guide for positive matrix factorization programs PMF2 and PMF3, Part2:
868 references. University of Helsinki, Helsinki, Finland, 2004b.

869

870 Pascal, M., Corso, M., Chanel, O., Declercq, C., Badaloni, C., Cesaroni, G., Henschel, S.,
871 Meister, K., Haluza, D., Martin-Olmedo, P. and Medina, S.: Assessing the public health
872 impacts of urban air pollution in 25 European cities: Results of the Aphekom project, *Sci.*
873 *Total Environ.*, 449(2007105), 390–400, doi:10.1016/j.scitotenv.2013.01.077, 2013.

874

875 Penza, M.: Low-cost sensors for outdoor air quality monitoring, Elsevier Inc., 2019.

876 Petkova, E. P., Jack, D. W., Volavka-Close, N. H. and Kinney, P. L.: Particulate matter
877 pollution in African cities, *Air Qual. Atmos. Heal.*, 6(3), 603–614, doi:10.1007/s11869-013-
878 0199-6, 2013.

879

880 Pokorná, P., Hovorka, J. and Hopke, P. K.: Elemental composition and source identification
881 of very fine aerosol particles in a European air pollution hot-spot, *Atmos. Pollut. Res.*, 7(4),
882 671–679, doi:10.1016/j.apr.2016.03.001, 2016.

883

884 Pope, F. D., Gatari, M., Ng'ang'a, D., Poynter, A. and Blake, R.: Airborne particulate matter

885 monitoring in Kenya using calibrated low cost sensors, *Atmos. Chem. Phys. Discuss.*, 1–31,
886 doi:10.5194/acp-2018-327, 2018.

887

888 Popoola, O. A. M., Carruthers, D., Lad, C., Bright, V. B., Mead, M. I., Stettler, M. E. J., Saffell,
889 J. R. and Jones, R. L.: Use of networks of low cost air quality sensors to quantify air quality in
890 urban settings, *Atmos. Environ.*, 194(February), 58–70,
891 doi:10.1016/j.atmosenv.2018.09.030, 2018.

892

893 Prakash, J., Choudhary, S., Raliya, R., Chadha, T., Fang, J., George, M. P. and Biswas, P.:
894 Deployment of Networked Low-Cost Sensors and Comparison to Real-Time Stationary
895 Monitors in New Delhi, *J. Air Waste Manage. Assoc.*, 0(0),
896 doi:10.1080/10962247.2021.1890276, 2021.

897

898 Raes, F., Dingenen, R. Van, Elisabetta, V., Wilson, J., Putaud, J. P., Seinfeld, J. H. and Adams,
899 P.: Formation and cycling of aerosols in the global troposphere, *Atmos. Environ.*, 34, 4215–
900 4240, 2000.

901

902 Reff, A., Eberly, S. I. and Bhawe, P. V.: Receptor Modeling of Ambient Particulate Matter Data
903 Using Positive Matrix Factorization: Review of Existing Methods, *J. Air Waste Manage.*
904 *Assoc.*, 57(2), 146–154, doi:10.1080/10473289.2007.10465319, 2007.

905

906 Rivas, I., Vicens, L., Basagaña, X., Tobías, A., Katsouyanni, K., Walton, H., Hüglin, C., Alastuey,
907 A., Kulmala, M., Harrison, R. M., Pekkanen, J., Querol, X., Sunyer, J. and Kelly, F. J.:
908 Associations between sources of particle number and mortality in four European cities,
909 *Environ. Int.*, 155(May), doi:10.1016/j.envint.2021.106662, 2021.

910

911 Schneider, P., Castell, N., Vogt, M., Dauge, F. R., Lahoz, W. A. and Bartonova, A.: Mapping
912 urban air quality in near real-time using observations from low-cost sensors and model
913 information, *Environ. Int.*, 106(May), 234–247, doi:10.1016/j.envint.2017.05.005, 2017.

914

915 Schnelle-Kreis, J., Sklorz, M., Orasche, J., Stölzel, M., Peters, A. and Zimmermann, R.: Semi
916 volatile organic compounds in ambient PM_{2.5}. Seasonal trends and daily resolved source

917 contributions, *Environ. Sci. Technol.*, 41(11), 3821–3828, doi:10.1021/es060666e, 2007.
918

919 Shafran-Nathan, R., Etzion, Y., Zivan, O. and Broday, D. M.: Estimating the spatial variability
920 of fine particles at the neighborhood scale using a distributed network of particle sensors,
921 *Atmos. Environ.*, 218(April), 117011, doi:10.1016/j.atmosenv.2019.117011, 2019.
922

923 Shindler, L.: Development of a low-cost sensing platform for air quality monitoring:
924 application in the city of Rome, *Environ. Technol. (United Kingdom)*, 42(4), 618–631,
925 doi:10.1080/09593330.2019.1640290, 2021.
926

927 Shiraiwa, M., Ueda, K., Pozzer, A., Lammel, G., Kampf, C. J., Fushimi, A., Enami, S., Arangio,
928 A. M., Fröhlich-Nowoisky, J., Fujitani, Y., Furuyama, A., Lakey, P. S. J., Lelieveld, J., Lucas, K.,
929 Morino, Y., Pöschl, U., Takahama, S., Takami, A., Tong, H., Weber, B., Yoshino, A. and Sato,
930 K.: Aerosol Health Effects from Molecular to Global Scales, *Environ. Sci. Technol.*, 51(23),
931 13545–13567, doi:10.1021/acs.est.7b04417, 2017.
932

933 Smith, K. R., Edwards, P. M., Ivatt, P. D., Lee, J. D., Squires, F., Dai, C., Peltier, R. E., Evans, M.
934 J., Sun, Y., and Lewis, A. C.: An improved low-power measurement of ambient NO₂ and O₃
935 combining electrochemical sensor clusters and machine learning, *Atmos. Meas. Tech.*, 12,
936 1325–1336, doi:10.5194/amt-12-1325-2019, 2019.
937

938 Sousan, S., Koehler, K., Thomas, G., Park, J. H., Hillman, M., Halterman, A. and Peters, T. M.:
939 Inter-comparison of low cost sensors for measuring the mass concentration of occupational
940 aerosols, *Aerosol Sci. Technol.*, 50(5), 462–473, doi:10.1080/02786826.2016.1162901, 2016.
941

942 Utsunomiya, A. and Wakamatsu, S.: Temperature and humidity dependence on aerosol
943 composition in the northern Kyushu, Japan, *Atmos. Environ.*, 30(13), 2379–2386,
944 doi:10.1016/1352-2310(95)00350-9, 1996.
945

946 Vajs, I., Drajić, D., Gligoric, N., Radovanovic, I. and Popovic, I.: Developing relative humidity
947 and temperature corrections for low-cost sensors using machine learning, *Sensors*, 21(10),
948 doi:10.3390/s21103338, 2021.

949

950 Valavanidis, A., Fiotakis, K. and Vlachogianni, T.: Airborne particulate matter and human
951 health: Toxicological assessment and importance of size and composition of particles for
952 oxidative damage and carcinogenic mechanisms, *J. Environ. Sci. Heal. - Part C Environ.*
953 *Carcinog. Ecotoxicol. Rev.*, 26(4), 339–362, doi:10.1080/10590500802494538, 2008.

954

955 Wang, P., Xu, F., Gui, H., Wang, H. and Chen, D. R.: Effect of relative humidity on the
956 performance of five cost-effective PM sensors, *Aerosol Sci. Technol.*, 55(8), 957–974,
957 doi:10.1080/02786826.2021.1910136, 2021.

958

959 Weissert, L., Alberti, K., Miles, E., Miskell, G., Feenstra, B., Henshaw, G. S., Papapostolou, V.,
960 Patel, H., Polidori, A., Salmond, J. A. and Williams, D. E.: Low-cost sensor networks and land-
961 use regression: Interpolating nitrogen dioxide concentration at high temporal and spatial
962 resolution in Southern California, *Atmos. Environ.*, 223(January), 117287,
963 doi:10.1016/j.atmosenv.2020.117287, 2020.

964

965 Whitty, R. C. W., Pfeffer, M. A., Ilyinskaya, E., Roberts, T. J., Schmidt, A., Barsotti, S., Strauch,
966 W., Crilley, L. R., Pope, F. D., Bellanger, H., Mendoza, E., Mather, T. A., Liu, E., Peters,
967 N., Taylor, I. A., Francis, H., Hernandez Leiva, X., Lynch, D., Nobert, S., Baxter, P.:
968 Effectiveness of low-cost air quality monitors for identifying volcanic SO₂ and PM downwind
969 from Masaya volcano, Nicaragua. *Volcanica*, 2022 (In press).

970

971 WHO global air quality guidelines. Particulate matter (PM_{2.5} and PM₁₀), ozone, nitrogen
972 dioxide, sulfur dioxide and carbon monoxide, World Health Organisation, ISBN 978-92-4-
973 003443-3, Licence: CC BY-NC-SA 3.0 IGO, Geneva, 2021

974

975 Wu, S., Ni, Y., Li, H., Pan, L., Yang, D., Baccarelli, A. A., Deng, F., Chen, Y., Shima, M. and Guo,
976 X.: Short-term exposure to high ambient air pollution increases airway inflammation and
977 respiratory symptoms in chronic obstructive pulmonary disease patients in Beijing, China,
978 *Environ. Int.*, 94, 76–82, doi:10.1016/j.envint.2016.05.004, 2016.

979

980 Xu, Y., Zhang, J.S.: Understanding SVOCs, *ASHRAE Journal*, 53 (12), 121 - 125, 2011.

981

982 Zeger, S. L., Dominici, F., McDermott, A. and Samet, J. M.: Mortality in the medicare
983 population and Chronic exposure to fine Particulate air pollution in urban centers (2000-
984 2005), *Environ. Health Perspect.*, 116(12), 1614–1619, doi:10.1289/ehp.11449, 2008.

985

986 **FIGURE LEGENDS**

987

988 **Figure 1:** Map of the measuring station.

989

990 **Figure 2:** Particle profiles of the factors from the PMF analysis (> 500 nm). The lines
991 indicate the average particle count per second for each particle size bin.

992

993 **Figure 3:** Variable association for the factors from the LC analysis. Grey bars indicate
994 the values of F, while red bars indicate the explained variations for each
995 variable.

996

997 **Figure 4:** Temporal variation of the contributions of the factors from the LC analysis. The
998 windroses refer to the wind conditions for the corresponding periods when
999 specific factors presented higher G contributions.

1000

1001 **Figure 5:** Polar plot of the average G contributions of the factors from the LC analysis.

1002

1003 **Figure 6:** Average G contribution of the factors from the LC analysis for incoming air
1004 masses. Higher contributions indicate better association of the given factor
1005 with the corresponding air mass origin.

1006

1007 **Figure 7:** Variable association for the factors from the RG analysis. Grey bars indicate the
1008 values of F, while red bars indicate the explained variations for each variable.

1009

1010 **Figure 8:** Polar plot of the average G contributions of the factors from the RG analysis.

1011

1012 **Figure 9:** Average G contribution of the factors from the RG analysis for incoming air
1013 masses. Higher contributions indicate better association of the given factor
1014 with the corresponding air mass origin.

1015

1016



1017

1018 Figure 1: Map of the measuring station. Imagery @2022 Bluesky, Getmapping plc, Infoterra

1019 Ltd & Bluesky, Maxar Technologies, The GoInformation Group, Map data

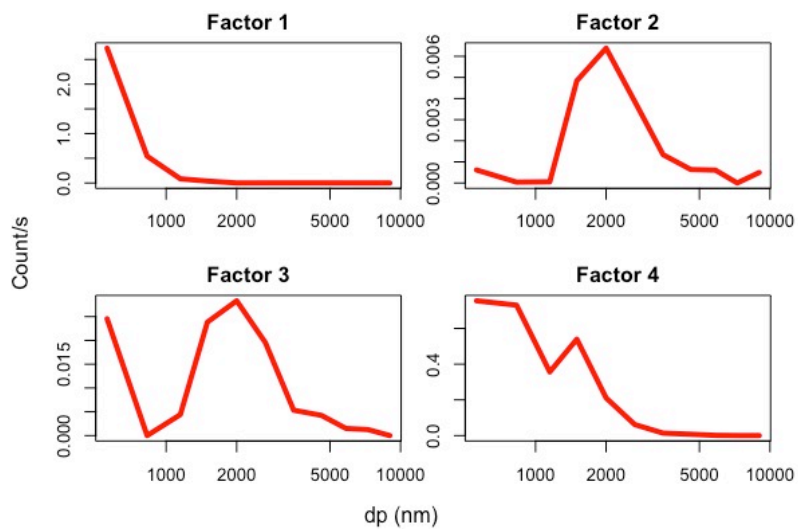
1020 ©2022

1021

1022

1023

1024

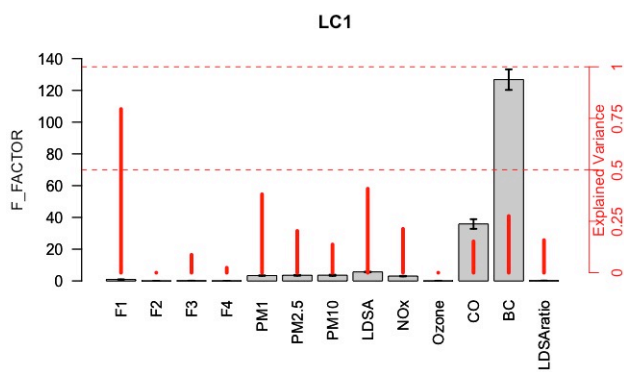


1025

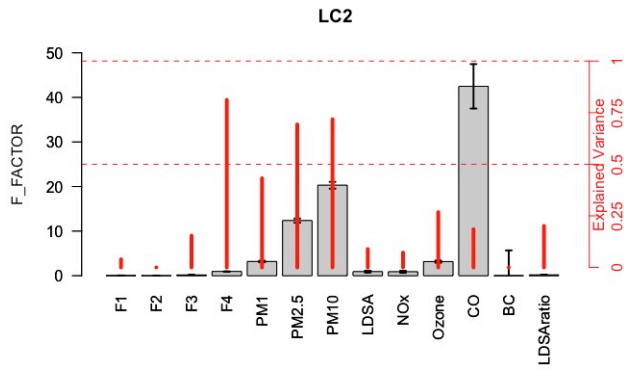
1026 Figure 2: Particle profiles of the factors from the PMF analysis (above 500 nm). The lines

1027 indicate the average particle count per second for each particle size bin.

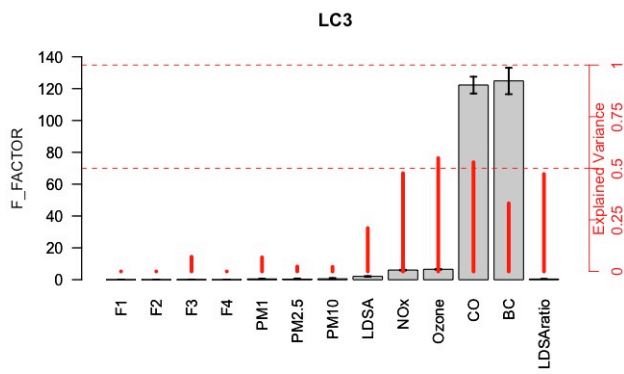
1028



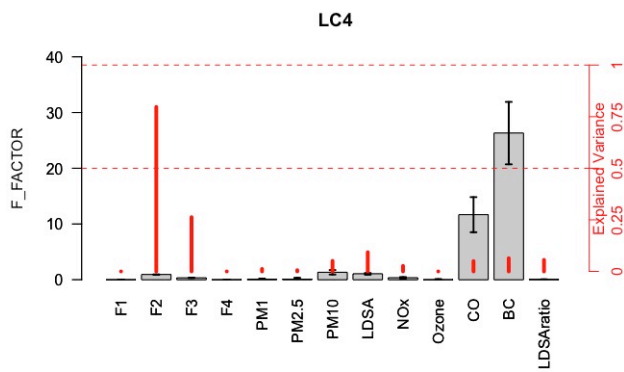
1029



1030



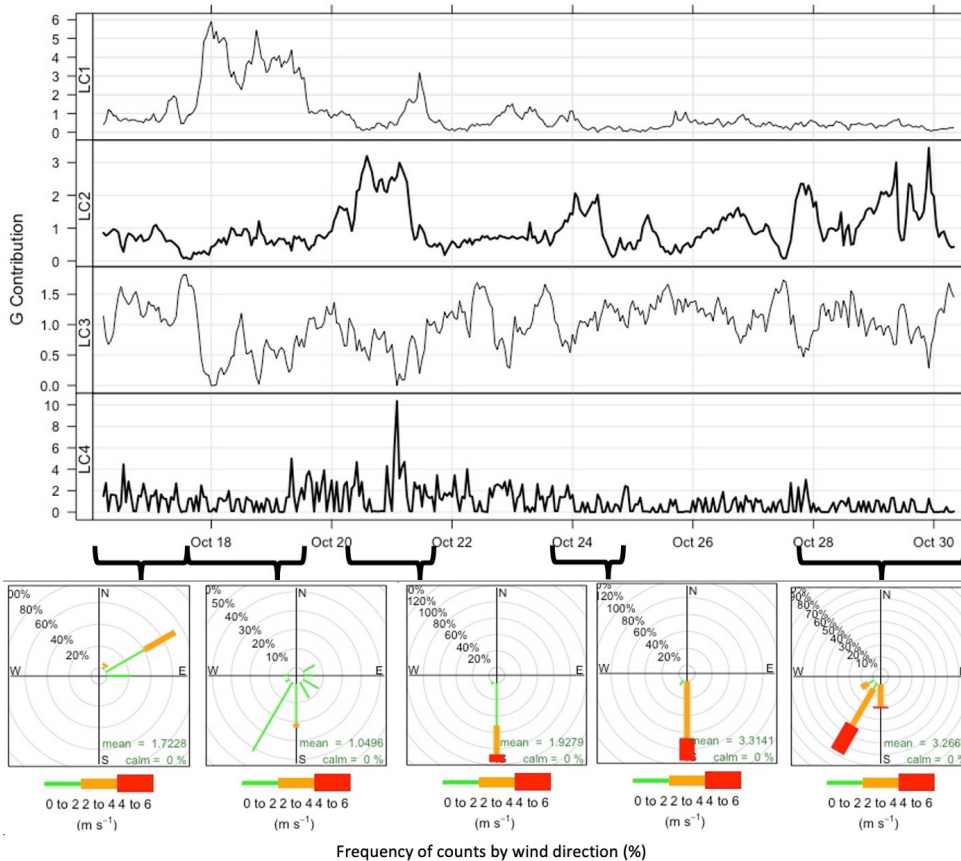
1031



1032

1033 Figure 3: Contribution of the factors from the LC analysis. Grey bars indicate the values of F,
 1034 while red bars indicate the explained variations for each variable.

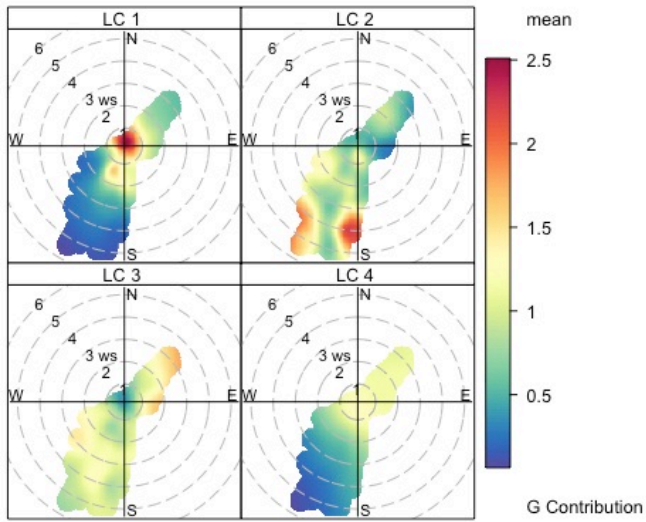
1035



1036

1037 Figure 4: Temporal variation of the contributions of the factors from the LC analysis. The
 1038 windroses refer to the wind conditions for the corresponding periods when specific factors
 1039 presented higher G contributions.

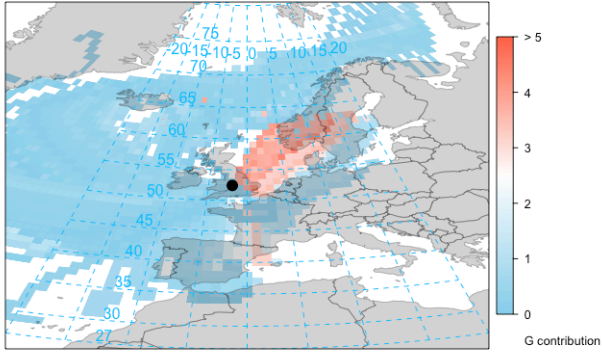
1040



1041

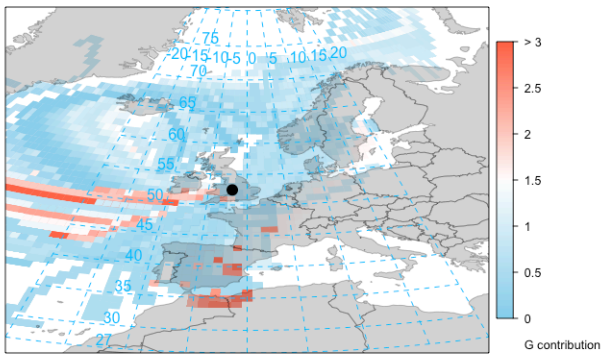
1042 Figure 5: Polar plot of the average G contributions of the factors from the LC analysis.

1043



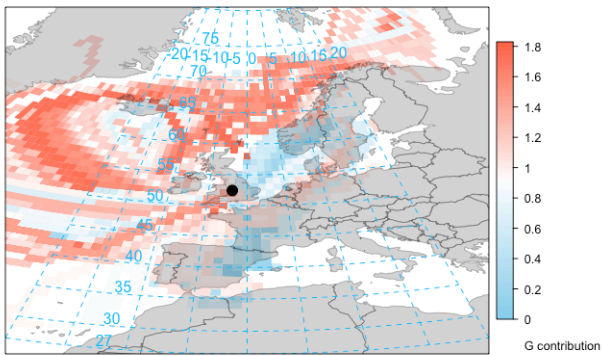
1044

LC1



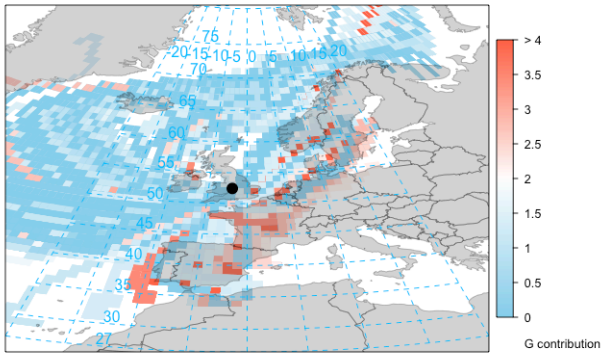
1045

LC2



1046

LC3



LC4

1047

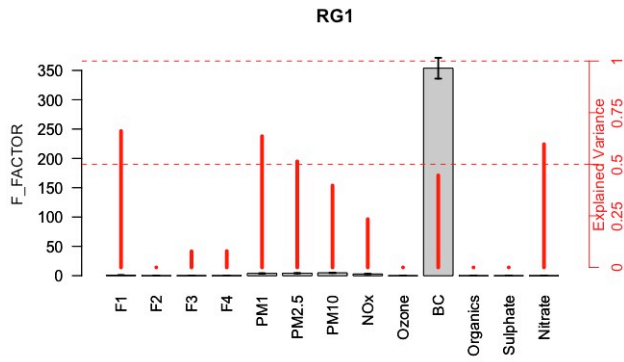
1048 Figure 6: Average G contribution of the factors from the LC analysis for incoming air masses.

1049 Higher contributions indicate better association of the given factor with the corresponding
 1050 air mass origin.

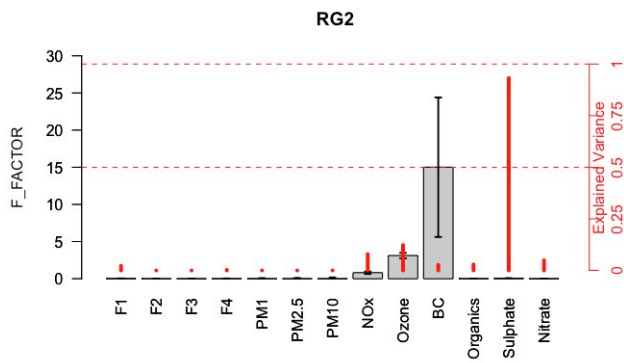
1051

1052

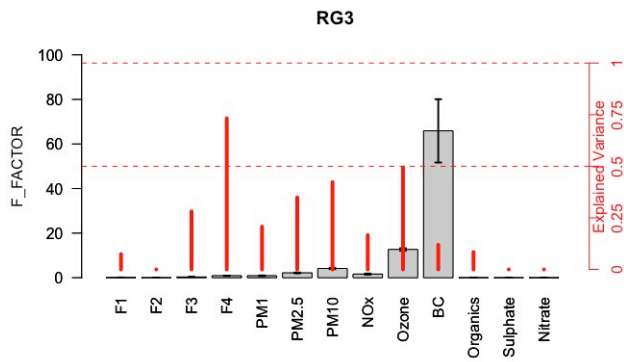
1053



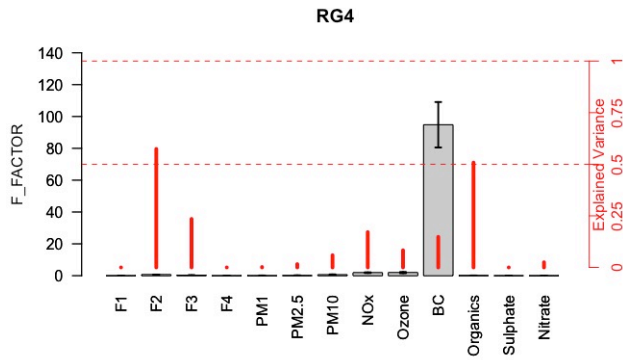
1054
1055



1056



1057

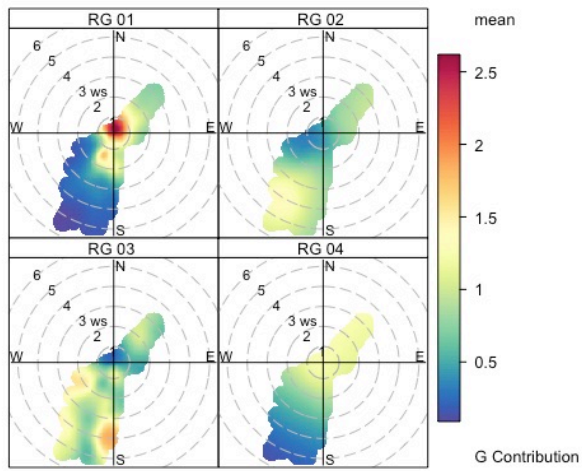


1058

1059 Figure 7: Variable association for the factors from the RG analysis. Grey bars indicate the
 1060 values of F, while red bars indicate the explained variations for each variable.

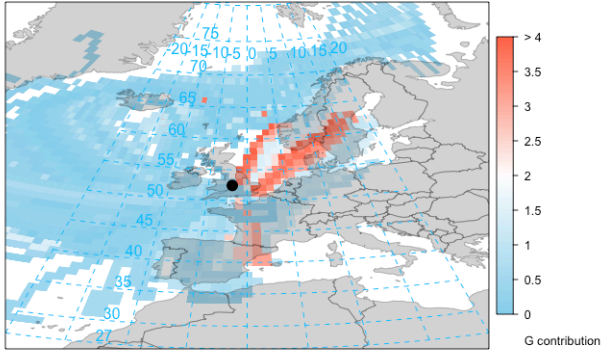
1061

1062



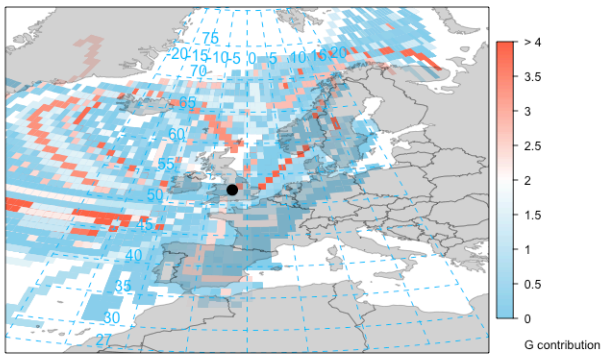
1063

1064 Figure 8: Polar plot of the average G contributions of the factors from the RG analysis.



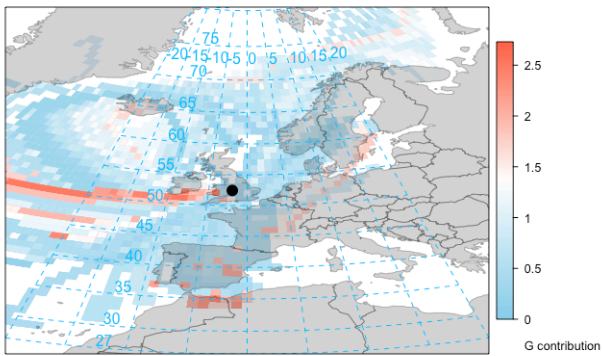
1065

RG1



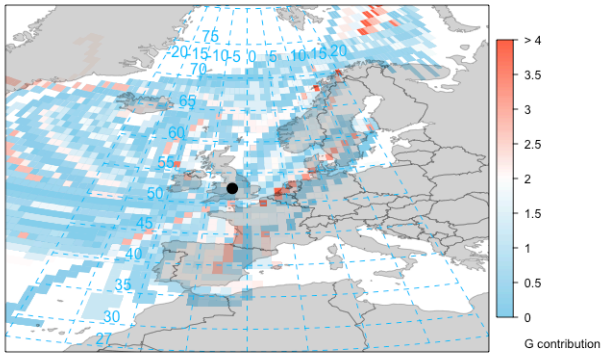
1066

RG2



1067

RG3



RG4

1068

1069 Figure 9: Average G contribution of the factors from the RG analysis for incoming air masses.

1070 Higher contributions indicate better association of the given factor with the corresponding

1071 air mass origin.